DiffScale: Towards continuous super-resolution in S2S wind forecasts

Maximilian Springenberg [1] Noelia Otero [1] Jackie Ma [1]

[1]Fraunhofer Heinrich-Hertz-Institute – Fraunhofer HHI, Berlin, Germany

Introduction: Motivation

Subseasonal to seasonal (S2S) forecasting bridges the gap between medium-range weather forecast (up to 10 days) and seasonal predictions (3–6 months). S2S forecasts are applied across various sectors including agriculture, water resource management and renewable energy, among others. Despite ongoing efforts and the potential for predictability, S2S forecasts exhibit limited skill, especially for surface variables. The skill of forecasting lead time for a weather event depends largely on its spatial scale, and improved resolutions are essential for achieving skillful S2S forecasts. In particular, the need for high-resolution wind resource information becomes crucial as the supply and development of wind power continue to expand. Here, we present Diffscale, a pots-processing deep learning approach based on diffusion models to downscale S2S forecast of wind surface. DiffScale is designed to super-resolve coarse-resolution S2S forecasts generated by the European Center for Medium-Range Weather Forecast (ECMWF).

Background & Implementation

In the score-based framework, we understand the diffusion process as an SDE

$$\mathrm{d}\mathbf{x} = f(t)\mathbf{x}\mathrm{d}t + g(t)\mathrm{d}\mathbf{w}_t, \tag{1}$$

with the reverse process

$$\mathrm{d}\mathbf{x} = \left[f(t)\mathbf{x} - g(t)^2\nabla_{\mathbf{x}}\log p_t(\mathbf{x}|c_1,\ldots,c_K)\right]\ \mathrm{d}t + g(t)\ \mathrm{d}\mathbf{w}_t, \tag{2}$$

where $\mathbf{w}$ is a standard wiener process, $c_1,\ldots,c_K$ are conditioning inputs that can guide the reverse process and $\nabla_{\mathbf{x}}\log p_t(\mathbf{x}|c_1,\ldots,c_K)$ can be approximated by a parameterized score function $s_\theta(\cdot|c_1,\ldots,c_K)$.

We choose a U-Net with attention in the bottleneck as the backbone for s_θ.

There are many solvers for eq. (2) (see [2]), in this work we use the simple Euler-Maruyama method. Furthermore we settle for the simple VE schedule with zero-drift

$$\sigma(t) = \sigma_{\min}\left(\frac{\sigma_{\max}}{\sigma_{\min}}\right)^t, \tag{3}$$

where we set $\sigma_{\min} = 0.01, \sigma_{\max} = 50$ and $t \sim \mathcal{U}[0,1]$ during training and inference (equidistant steps).

Data: ECMWF reforecast and reanalysis

The forecast and retrospective forecast (reforecast) data are derived from the European Centre for Medium-Range Weather Forecasts (ECMWF), accessible via the Subseasonal-to-Seasonal (S2S) Prediction Project Database [3]. Atmospheric variables, namely 2m surface temperature, mean sea level pressure, zonal wind (u), meridional wind (v) at 300, 925 hPa, geopotential at 500 hPa and 10m wind speed are used as input data. Additionally, high-resolution orography data is included in the inputs. The high-resolution 10m wind speed used as our target is retrieved from the ERA5 reanalysis [1].

- **Forecast** are the operational ensemble predictions consisting of 51 members (50 perturbed 1 control). The real time forecasts correspond to the year 2021, including model cycles Cy47r1, Cy47r2, and Cy47r3, switching in May and then October of 2021, respectively. Here, the forecast are used only for testing purposes.
- **Reforecast** from ECMWF are computed twice a week (Mondays and Thursdays) and consist of 11 ensemble members (10 perturber + 1 control), covering a forecast lead time up to 46 days and with a spatial resolution of 1.5°. The reforecast data spans from 2001 to 2020. In this study, only the perturbed members of both forecasts and reforecasts are utilized.
- **ERA5** reanalysis data serves as the reference. The data has been retrieved at its original spatial resolution (0.25°).

Method

As a proof of concept, we use a lead time of one day in our experiments, which are conducted over Germany, covering the area from 0 ° to 27 ° logitude and 45 ° to 53 ° latitude. We condition the diffusion model with the ensemble means of a numerical model, rather than a lower resolution version of the ground truth target. The ensemble inputs do not always match the ground truth (see fig. 3), hence we add additional prior knowledge as conditioning input.

To achieve super-resolution for different scaling factors (without re-applying the model), we additionaly embed the scaling factor s as a conditioning input. This helps the model achieve continuous super-resolution w.r.t. s.

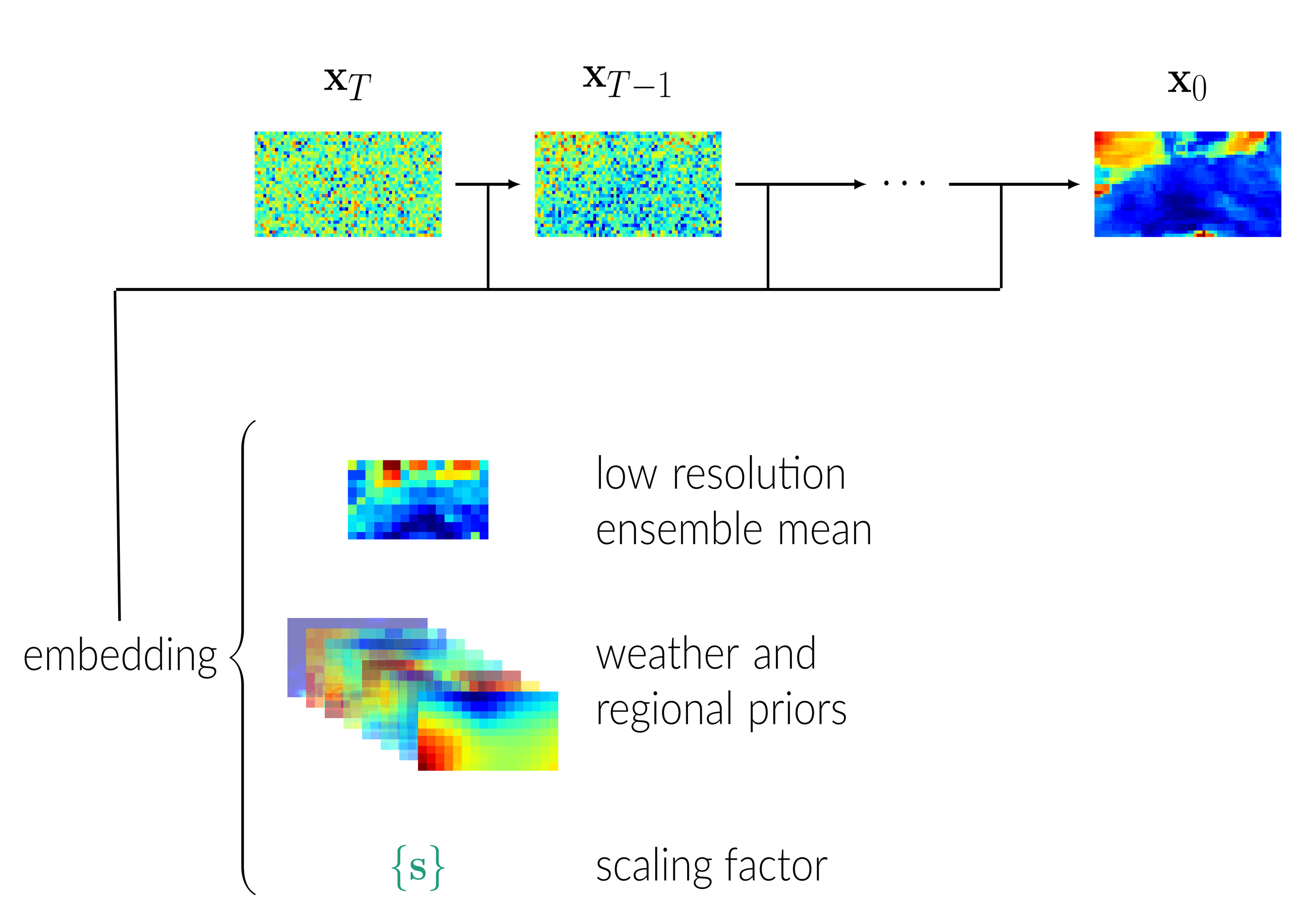

Figure 1. Sampling from our Diffusion Model with conditioning inputs. Transitions with an arrow are performed via the Euler-Maruyama method, given our score function s_θ.

Results

We achieve a significant increase in the prediction quality (see table 1), utilizing our diffusion model that handles both: continuous super-resolution and bias correction of the ensemble mean. For our predictions we sampled from the same diffusion model 10 times with the same inputs.

Figure 2 shows how the model has learned to upsample by arbitrary scaling factors s. The diffusion model allows for more variation of sample outputs, yielding corrected predictions. Figures 4 to 7 show how the model handles bias correction with more variation in its predictions, to account for uncertainty.

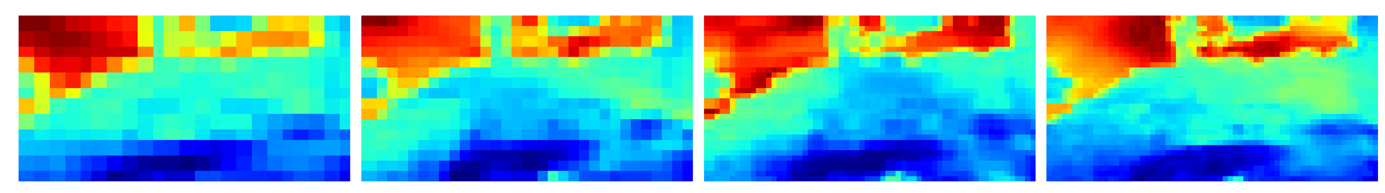

(a) $\times 1$ (b) $\times 2$ (c) $\times 3$ (d) $\times 4$

Figure 2. Continuous Super-Resolution. Displayed are the means over 10 predictions obtained from the same diffusion model, with respective conditioning input s.

Scaling Factor (s)	CRPS Loss ↓		
	Ensemble Input	Ensemble Input (Interp.)	DiffScale
$\times 4$	0.691 ± 0.673	0.689 ± 0.656	$\mathbf{0.536 \pm 0.328}$
$\times 3$	0.686 ± 0.668	0.685 ± 0.652	$\mathbf{0.536 \pm 0.348}$
$\times 2$	0.682 ± 0.665	0.682 ± 0.647	$\mathbf{0.534 \pm 0.331}$
$\times 1$	0.682 ± 0.664	0.678 ± 0.646	$\mathbf{0.529 \pm 0.328}$

Table 1. CRPS with normalized data. First column: raw Ensemble inputs of the numerical model, second column interpolated (upsampled via bilinear interpolation) Ensemble inputs of the numerical model, third column: our diffusion model.

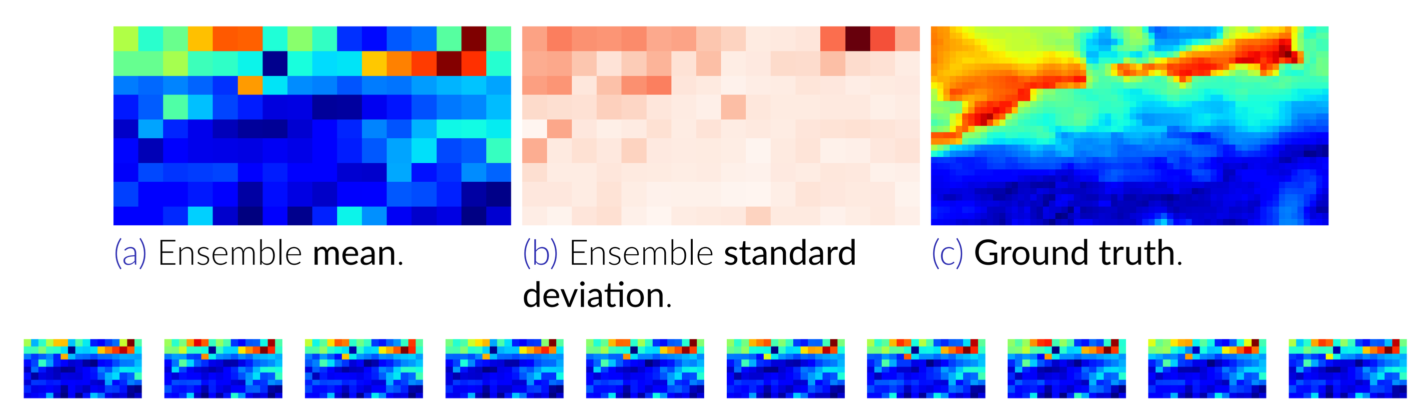

(a) Ensemble **mean**. (b) Ensemble **standard deviation**. (c) **Ground truth**.

(d) Ensemble inputs.

Figure 3. Bias of ensemble **input**.

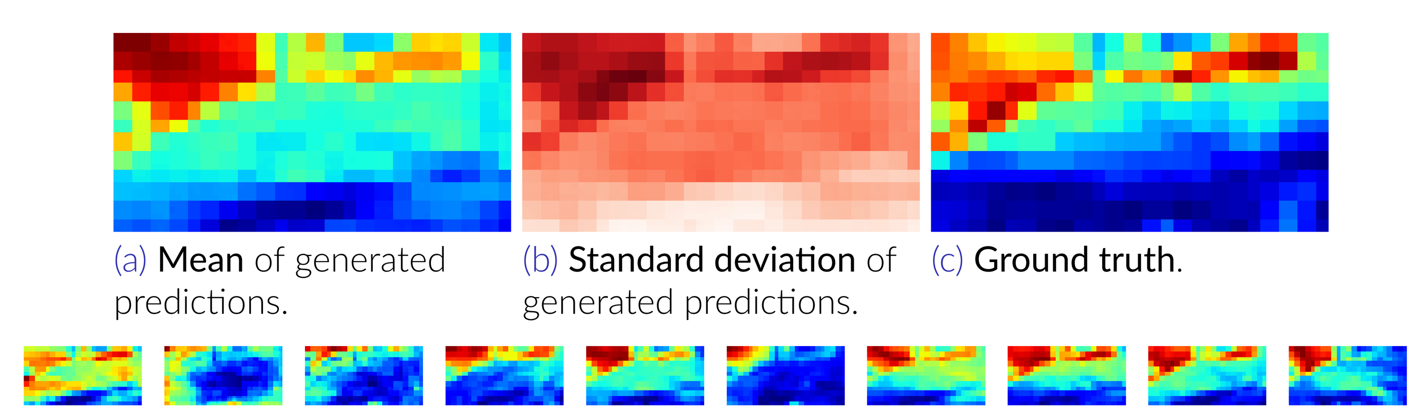

(a) **Mean** of generated predictions. (b) **Standard deviation** of generated predictions. (c) **Ground truth**.

(d) Generated predictions.

Figure 4. Bias correction of generated **predictions** $(\times 1)$.

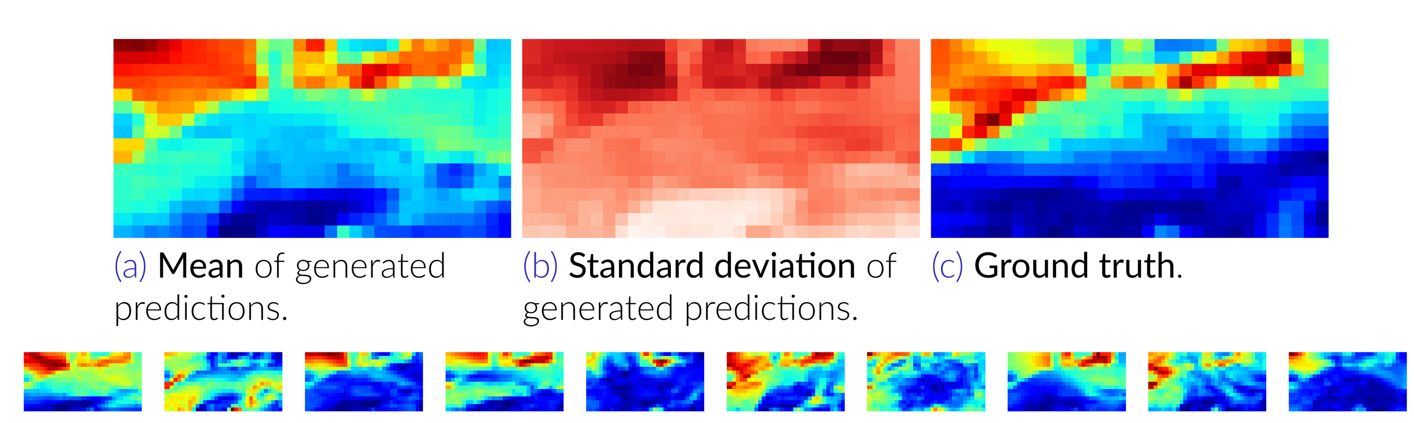

(a) **Mean** of generated predictions. (b) **Standard deviation** of generated predictions. (c) **Ground truth**.

(d) Generated predictions.

Figure 5. Bias correction of generated **predictions** $(\times 2)$.

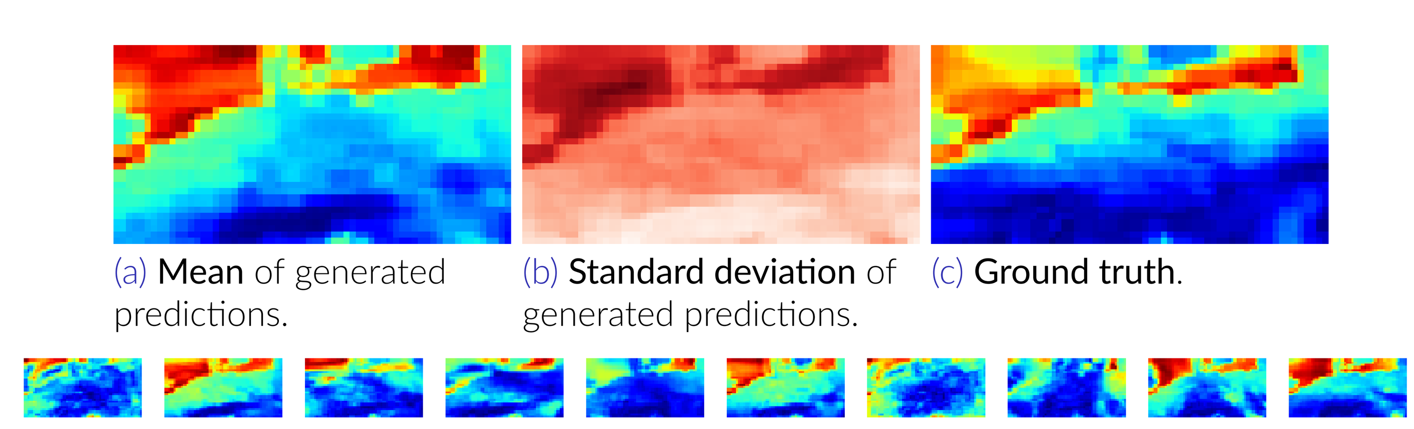

(a) **Mean** of generated predictions. (b) **Standard deviation** of generated predictions. (c) **Ground truth**.

(d) Generated predictions.

Figure 6. Bias correction of generated **predictions** $(\times 3)$.

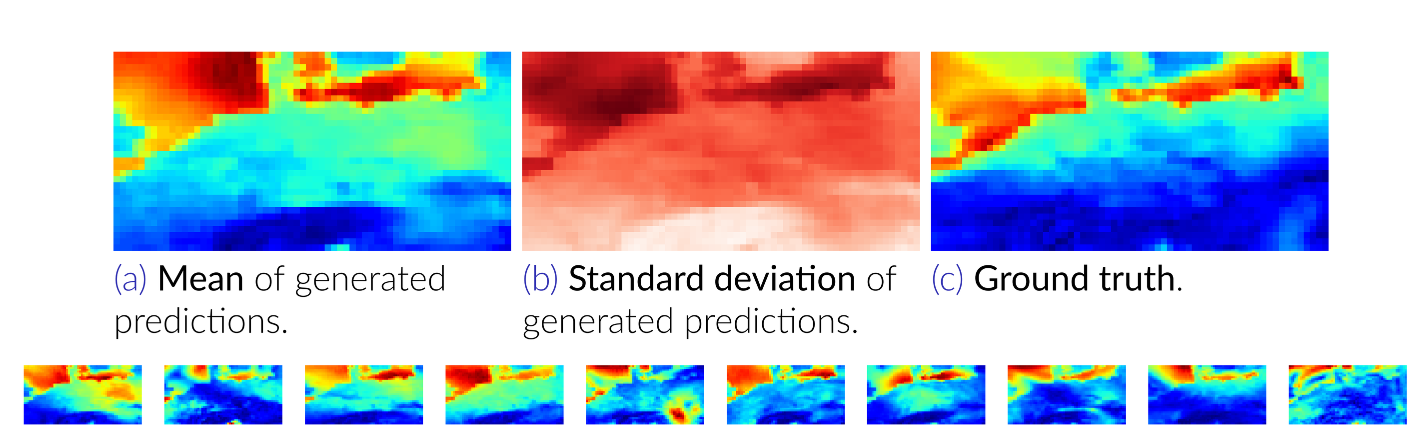

(a) **Mean** of generated predictions. (b) **Standard deviation** of generated predictions. (c) **Ground truth**.

(d) Generated predictions.

Figure 7. Bias correction of generated **predictions** $(\times 4)$.

References

[1] Hans Hersbach, Bill Bell, Paul Berrisford, Shoji Hirahara, András Horányi, Joaquín Muñoz-Sabater, Julien Nicolas, Carole Peubey, Raluca Radu, Dinand Schepers, Adrian Simmons, Cornel Soci, Saleh Abdalla, Xavier Abellan, Gianpaolo Balsamo, Peter Bechtold, Gionata Biavati, Jean Bidlot, Massimo Bonavita, Giovanna De Chiara, Per Dahlgren, Dick Dee, Michail Diamantakis, Rossana Dragani, Johannes Flemming, Richard Forbes, Manuel Fuentes, Alan Geer, Leo Haimberger, Sean Healy, Robin J. Hogan, Elías Hólm, Marta Janisková, Sarah Keeley, Patrick Laloyaux, Philippe Lopez, Cristina Lupu, Gabor Radnoti, Patricia de Rosnay, Iryna Rozum, Freja Vamborg, Sebastien Villaume, and Jean-Noël Thépaut. The era5 global reanalysis. *Quarterly Journal of the Royal Meteorological Society*, 146(730):1999–2049, 2020.

[2] Tero Karras, Miika Aittala, Timo Aila, and Samuli Laine. Elucidating the design space of diffusion-based generative models. In *Proc. NeurIPS*, 2022.

[3] F. Vitart, C. Ardilouze, A. Bonet, A. Brookshaw, M. Chen, C. Codorean, M. Déqué, L. Ferranti, E. Fucile, M. Fuentes, H. Hendon, J. Hodgson, H.-S. Kang, A. Kumar, H. Lin, G. Liu, X. Liu, P. Malguzzi, I. Mallas, M. Manoussakis, D. Mastrangelo, C. MacLachlan, P. McLean, A. Minami, R. Mladek, T. Nakazawa, S. Najm, Y. Nie, M. Rixen, A. W. Robertson, P. Ruti, C. Sun, Y. Takaya, M. Tolstykh, F. Venuti, D. Waliser, S. Woolnough, T. Wu, D.-J. Won, H. Xiao, R. Zaripov, and L. Zhang. The subseasonal to seasonal (s2s) prediction project database. *Bulletin of the American Meteorological Society*, 98(1):163 – 173, 2017.